ELSEVIER

Deposit morphology of the zinc recovery by electrodeposition from the spent Zn–MnO$_2$ batteries

M.B.J.G. Freitas*, M.K. de Pietre

*Universidade Federal do Espírito Santo, Departamento de Química, Laboratório de Eletroquímica Aplicada,
Av. Fernando Ferrari s/n, Goiabeiras, Vitória CEP 29060-900, ES, Brasil*

Abstract

Electrochemical recovery of zinc from spent Zn–MnO$_2$ batteries has been developed. Deposit morphology and charge efficiency depends on current density. A smooth deposit is formed for a current density equal to 50.0 mA cm^{-2}, while a porous deposit is formed for a current density equal to 10.0 mA cm^{-2}. It was observed that pore size decreases with the increase in current density. In contrast, charge efficiency reaches up to 85.0% for a current density equal to 10.0 mA cm^{-2}, and decreases with further increase in current density. Potassium, sulphur, and oxygen are adsorbed onto the zinc deposit. Zinc recovery was analyzed by scanning electron microscopy (SEM) and energy dispersive X-ray analysis (EDX).
© 2004 Elsevier B.V. All rights reserved.

Keywords: Recycling; Zinc recovery; Spent battery; Zinc; Electrochemical recycling

1. Introduction

Secondary alkaline batteries such as Ni–Cd and Ni–MH are used in applications that require high energy density, long useful life, and high discharge rates. Lithium batteries present great energy density, but they are the most expensive ones [1]. Zn–MnO$_2$ primary batteries are used in applications that require low energy density and short useful life [2,3]. In Brazil, about 1 billion Zn–MnO$_2$ batteries are used annually [4,5]. Discharged Zn–MnO$_2$ batteries can be discarded with domestic garbage in a municipal landfill [6]. The growing disposal of spent Zn–MnO$_2$ batteries has become a serious environmental problem. Recycling is a possible solution for this environmental problem [7]. Hydrometallurgical recycling of zinc from spent batteries does not pollute and contributes to the preservation of natural resources. Recovered zinc electrodeposited onto steel iron–carbon 1020 serves as a protection against corrosion [8]. Steel galvanization is extensively used

in metallurgical industries. The efficiency of the zinc deposit in the protection of steel against corrosion depends on deposit morphology, which is related with the composition of the electrodeposition bath and current density. The present work reports on the development of electrochemical recovery of zinc from spent Zn–MnO$_2$ batteries. The relation between current density and deposit morphology was analyzed. The materials obtained under different electrodeposition conditions were analyzed by scanning electron microscopy (SEM) and energy dispersive X-ray analysis (EDX).

2. Experimental

2.1. Mechanical process

A mini-pilot plant for recycling spent Zn–MnO$_2$ batteries was built in the laboratory. The battery recycling process requires selective collection conditions, appropriate dismantling, and a sequence of physical and electrochemical transformations. In the selective collection, spent batteries were
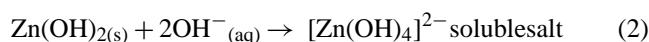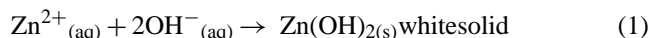
* Corresponding author. Tel.: +55 27 33352486; fax: +55 27 33352460.
  E-mail address: marcosbj@hotmail.com (M.B.J.G. Freitas).

sorted out in homogeneous lots. Spent type AA "mercury free" Zn–MnO$_2$ primary batteries produced by Panasonic were used in this research. In dismantling, spent batteries are physically separated into their different parts, anode, cathode material (MnO$_2$ and graphite), and steel (separators and current collectors). On average, the anode corresponds from 18.0 to 21.0% of the total weight of Zn–MnO$_2$ batteries.

2.2. Preparation of leaching and alkaline bath

Anode dissolution was in the proportion of 1.0 g of anode material to each 100 mL of H$_2$SO$_4$ 0.5 mol L^{-1} solution. The suspension was maintained under constant stirring at 298 K. Under these conditions, complete dissolution took 7 days. The suspension was filtered after anode leaching. Solution pH before and after anode dissolution was equal to 0.737 and 0.883, respectively. The difference in the amount of H$_2$SO$_4$ (mol) before and after anode dissolution is equivalent to the amount of Zn^{2+} in the leaching solution. The concentration of ionic zinc in the leaching solution was equal to

0.1413 mol L^{-1}. To prepare the alkaline bath, a solution of KOH 6.0 mol L^{-1} was added to the leaching solution. Acid neutralization occurred for pH lower than 6.0. In the pH interval between 6.0 and 7.5, the precipitation of zinc hydroxide occurred. The precipitated zinc hydroxide is dissolved in pH higher than 13. The reaction can be written as follows:

$$Zn^{2+}_{(aq)} + 2OH^-_{(aq)} \rightarrow Zn(OH)_{2(s)} \text{white solid} \tag{1}$$

$$Zn(OH)_{2(s)} + 2OH^-_{(aq)} \rightarrow [Zn(OH)_4]^{2-} \text{soluble salt} \tag{2}$$

2.3. Electrochemical cell

Working electrodes with a geometric area of 0.20 cm^2 were made from a rectangular sheet of steel 1020. The auxiliary electrode with a geometric area of 3.75 cm^2 was made from a platinum sheet. The reference electrode was Ag/AgCl/NaCl (saturated). Before each electrochemical experiment, the working electrodes were sanded with 600-grit sandpaper and then rinsed with distilled water. The
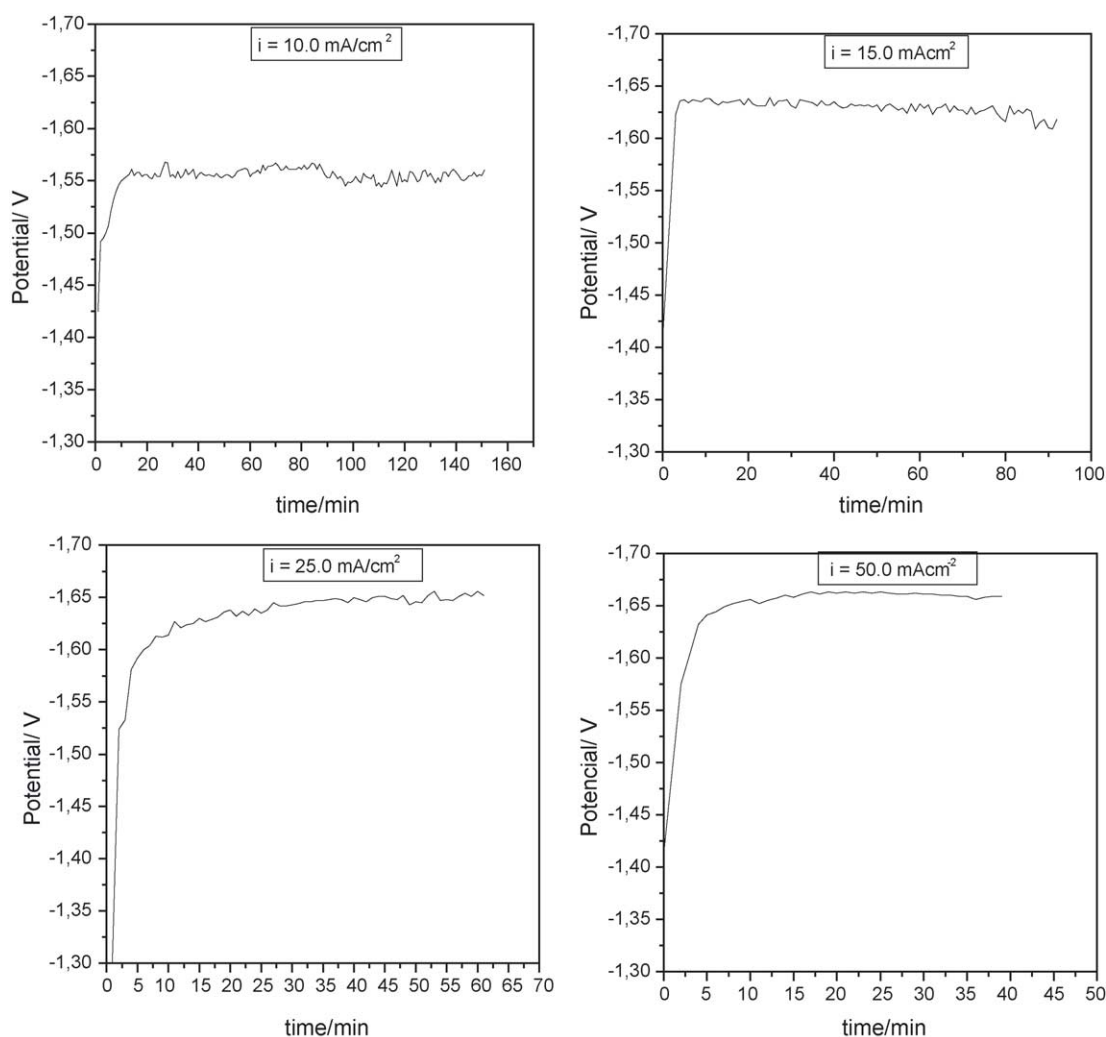

Fig. 1. Chronopotentiometric plot for ionic zinc electrodeposition in alkaline solution, $q_{applied} = 90.0$ C cm^{-2}, 298 K, without stirring.

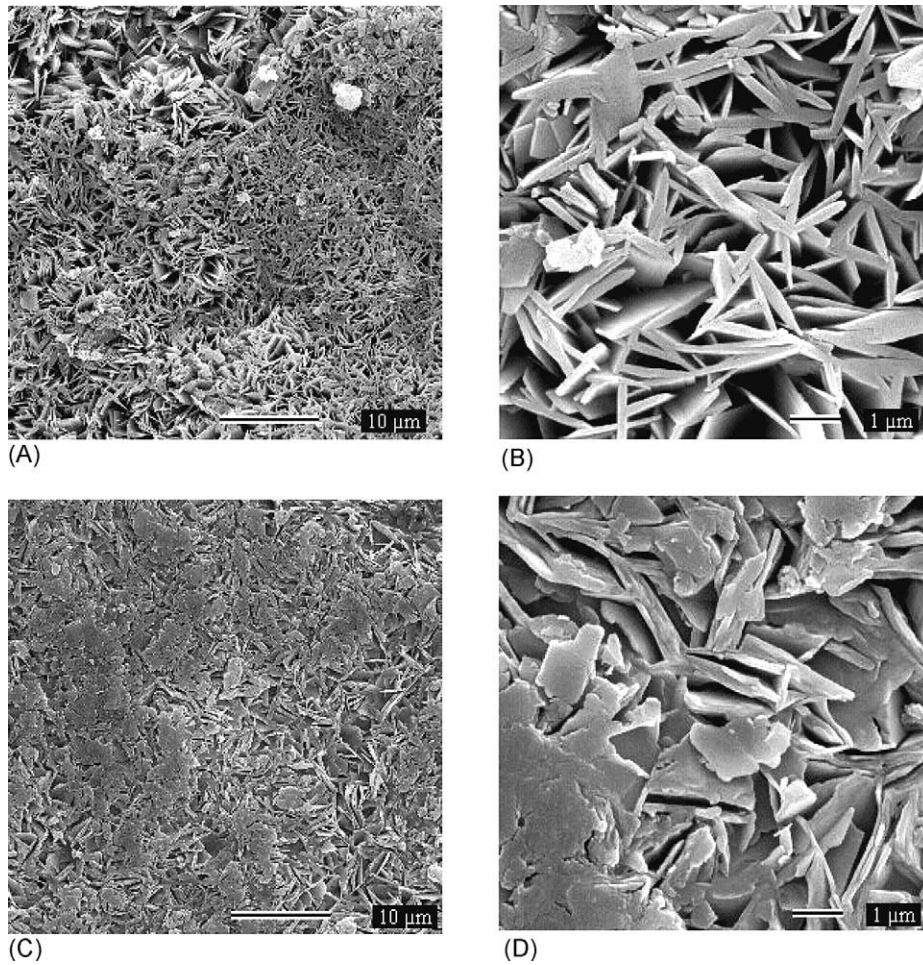Fig. 2. Typical scanning electron microscopy for zinc electrodeposit: (A) $i = 10.0\,\mathrm{mA\,cm^{-2}}$ and $2000\times$; (B) $i = 10.0\,\mathrm{mA\,cm^{-2}}$ and $10,000\times$; (C) $i = 50.0\,\mathrm{mA\,cm^{-2}}$ and $2000\times$; (D) $i = 50.0\,\mathrm{mA\,cm^{-2}}$ and $10,000\times$; $q_{applied} = 90.0\,\mathrm{C\,cm^{-2}}$.
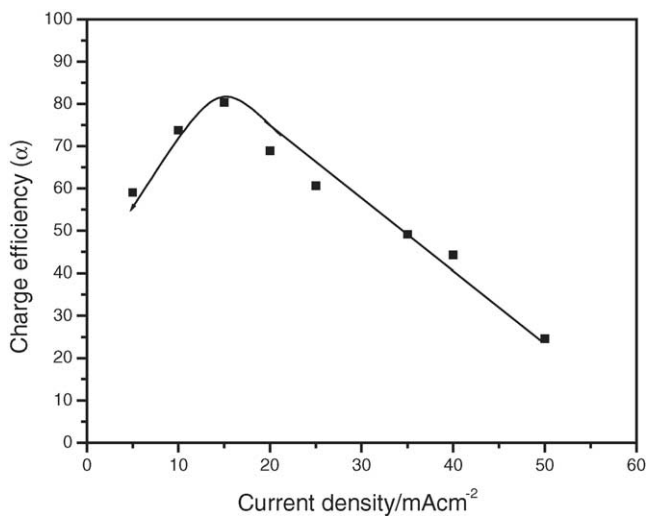

Fig. 3. Charge efficiency in function of the current density for zinc electrodeposition in alkaline solution, $q_{applied} = 90.0\,\mathrm{C\,cm^{-2}}$, 298 K, without stirring.

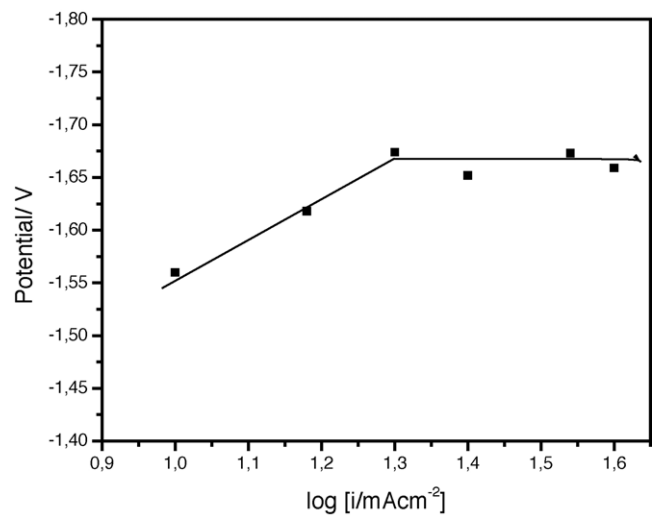Fig. 4. Potential in function of the logarithmic of the current density for zinc electrodeposition in alkaline solution, $q_{applied} = 90.0\,\mathrm{C\,cm^{-2}}$, 298 K, without stirring.
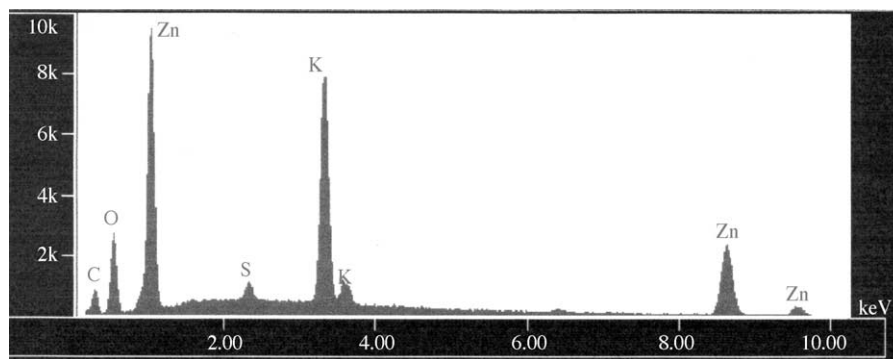
Fig. 5. Typical energy dispersive analysis of X-ray for zinc electrodeposition, $i = 50.0 \, \mathrm{mA \, cm^{-2}}$, $q_{\mathrm{applied}} = 90.0 \, \mathrm{C \, cm^{-2}}$, 298 K, without stirring.

galvanostatic experiments were performed with a regulated power supply built in the laboratory. The work and the auxiliary electrodes were connected to the voltmeter and connected to a microcomputer by a RS232 interface. The electrolytic solutions were prepared with reagent p.a. and pure water. The solutions were changed after each experiment. All electrochemical experiments were performed at 298 K.

2.4. Characterization techniques

The following techniques were used for material characterization: scanning electron microscopy (SEM), and energy dispersive X-ray analysis (EDX). SEM and EDX analysis were carried out with JEOL JXA, model 8900RL, equipped with an energy dispersive X-ray detector. The samples were covered with carbon for EDX analysis, and afterwards, covered with gold for obtaining SEM microphotographs.

3. Results and discussion

The crystallization process of the zinc deposit begins with the growth of nuclei. The rate and the direction of nucleus growth depend on current density. Therefore, there is a correlation between current density and coating morphology [9]. Oscillations in the reaction potential can be seen in the chronopotentiometric plot shown in Fig. 1. Potential oscillation frequency decreases with the increase in current density. These oscillations appear as a result of the irregular growth of metallic zinc. For high current densities, the nucleus radius growth rate in a direction parallel to the electrode surface is larger than that in other directions. In this case, microporosity decreases and the macropore extension between the agglomerates is smaller. For low current densities, the nucleus radius growth rate perpendicularly to the electrode surface is larger than in other directions. In this case, the nucleus radii do not overlap, and thus the crystal agglomerates present large microporosity. Fig. 2 shows SEM micrographs of the zinc deposit.

As can be seen in Fig. 3, the current density affects not only deposit morphology but also electrodeposition charge efficiency. Charge efficiency decreases with the increase in current density. This happens because hydrogen evolution on metallic zinc increases when current density increases.

The reaction potential (measured for a constant charge density) as a function of the logarithmic of the current density (Fig. 4) demonstrates that zinc electrodeposition kinetics mechanism changes. It is activation controlled for current densities lower than $20.0 \, \mathrm{mA \, cm^{-2}}$, and becomes mass-transport controlled for current densities higher than $20.0 \, \mathrm{mA \, cm^{-2}}$.

EDX analysis shows that independently from current density, potassium, sulphur, and oxygen are adsorbed onto the zinc deposit. Potassium and sulphur are from the solution. The oxygen detected may either come from the electrolytic solution or result of the growth of pre-existing film on metallic zinc. Fig. 5 is a typical example of EDX for zinc deposit.

4. Conclusions

There is a correlation between current density and zinc deposit morphology. Oscillations in the reaction potential in the chronopotentiometric plot appear as the result of irregular growth of metallic zinc. Scanning electron microscopy of the zinc deposit showed that for low current density, the crystal agglomerates show microporosity, while for high current density, microporosity and the extension of macropores between agglomerates are smaller. Current density affects not only deposit morphology but also electrodeposition charge efficiency. Parallel reactions such as hydrogen evolution reduce the charge efficiency of recovery of zinc from alkaline solution. Zinc electrodeposition is activation controlled for current densities lower than $20.0 \, \mathrm{mA \, cm^{-2}}$, and becomes mass-transport controlled for current densities higher than $20.0 \, \mathrm{mA \, cm^{-2}}$. EDX analysis showed that potassium, sulphur and oxygen are adsorbed onto zinc deposit.

References

[1] C.J. Rydh, B. Svärd, Sci. Total Environ. 302 (2003) 167.
[2] N. Vatistas, M. Bartolozzi, J. Power Sources 79 (1999) 199.
[3] N. Vatistas, M. Bartolozzi, S. Arras, J. Power Sources 101 (2001) 182.
[4] A.M. Bernardes, D.C.R. Espinosa, J.A.S. Tenorio, J. Power Sources 124 (2004) 586.
[5] A.M. Bernardes, D.C.R. Espinosa, J.A.S. Tenorio, J. Power Sources 130 (2004) 291.
[6] CONAMA (CONSELHO NACIONAL DO MEIO AMBIENTE) which is the Brazilian Environmental Council, Resolution no. 257, June 30, 1999.
[7] H.P. Fahri, J. Power Sources 57 (1995) 47.
[8] M.B.J.G. Freitas, M.K. de Pietre, J. Power Sources 128 (2004) 343.
[9] M.B.J.G. Freitas, S.F. Rosalém, J. Power Sources 139 (2005) 366.